

REPORT DOCUMENTATION PAGE

Form Approved
OMB No. 0704-01-0188

The public reporting burden for this collection of information is estimated to average 1 hour per response, including the time for reviewing instructions, searching existing data sources, gathering and maintaining the data needed, and completing and reviewing the collection of information. Send comments regarding this burden estimate or any other aspect of this collection of information, including suggestions for reducing the burden to Department of Defense, Washington Headquarters Services Directorate for Information Operations and Reports (0704-0188), 1215 Jefferson Davis Highway, Suite 1204, Arlington VA 22202-4302. Respondents should be aware that notwithstanding any other provision of law, no person shall be subject to any penalty for failing to comply with a collection of information if it does not display a currently valid OMB control number.

PLEASE DO NOT RETURN YOUR FORM TO THE ABOVE ADDRESS.

1. REPORT DATE (DD-MM-YYYY) 13-08-2010		2. REPORT TYPE REPRINT		3. DATES COVERED (From - To)	
4. TITLE AND SUBTITLE Effect of Aspect Ratio on the Wettability and Electrospray Properties of Porous Tungsten Emitters with the Ionic Liquid [Emim][Im]				5a. CONTRACT NUMBER	
				5b. GRANT NUMBER	
				5c. PROGRAM ELEMENT NUMBER 61102F	
6. AUTHORS Brian W. Ticknor, Julie K Anderson, Bruce A. Fritz and Yu-Hui Chiu				5d. PROJECT NUMBER 2303	
				5e. TASK NUMBER RS	
				5f. WORK UNIT NUMBER A1	
7. PERFORMING ORGANIZATION NAME(S) AND ADDRESS(ES) Air Force Research Laboratory /RVBXT 29 Randolph Road Hanscom AFB, MA 01731-3010				8. PERFORMING ORGANIZATION REPORT NUMBER AFRL-RV-HA-TR-2010-1081	
9. SPONSORING/MONITORING AGENCY NAME(S) AND ADDRESS(ES)				10. SPONSOR/MONITOR'S ACRONYM(S) AFRL/RVBXT	
				11. SPONSOR/MONITOR'S REPORT NUMBER(S)	
12. DISTRIBUTION/AVAILABILITY STATEMENT Approved for public release; distribution unlimited.					
13. SUPPLEMENTARY NOTES Reprinted From: Proceedings, 46 th AIAA/ASE/SAE/ASEE Joint Propulsion Conference & Exhibit, 25-28 July 2010, Nashville, TN					
14. ABSTRACT Porous tungsten emitters of different aspect ratios, produced by a novel electrochemical etching process, are studied by angle-resolved mass spectrometry and retarding potential energy analysis, which provides information on the mechanisms of ion field evaporation and spatial distributions of the emitted ions and droplets. In the present study, the ionic liquid [Emim][Im] (1-ethyl-3-methylimidazolium bis(trifluoromethylsulfonyl)imide) is sprayed from two externally wetted porous tungsten emitters. Near field current and mass flow measurements show that while both emitters operate in a mixed ion-droplet mode, the longer 3 mm emitter has a slower liquid flow rate than the shorter, 2 mm emitter. The mass spectrometric analysis shows that the 3 mm emitter favors the production of smaller ions, while the mass distribution shifts to larger clusters with the use of the 2 mm emitter. The ion energy analysis suggests that all of the observed ions and droplets, from both emitters, have energies near that of the emitter potential, seemingly indicating that they are all formed in the neck region of the Taylor cone. The combined near field and mass spectrometry results are consistent with the observation that the shorter emitter supports a larger liquid flow rate to the tip than that produced from the longer emitter, leading to emission that contains a larger fraction of droplets versus ions, and also produces droplets of a larger size.					
15. SUBJECT TERMS Electrospray thruster Ionic liquid Mass spectrometry Externally wetted porous tungsten emitter 1-ethyl-3-methylimidazolium bis(trifluoromethylsulfonyl)imide, [Emim] [Im]					
16. SECURITY CLASSIFICATION OF:			17. LIMITATION OF ABSTRACT	18. NUMBER OF PAGES	19a. NAME OF RESPONSIBLE PERSON
a. REPORT	b. ABSTRACT	c. THIS PAGE			Yu-Hui Chiu
UNCL	UNCL	UNCL	UNL	12	19b. TELEPHONE NUMBER (Include area code)

DTIC COPY

Effect of Aspect Ratio on the Wettability and Electro spray Properties of Porous Tungsten Emitters with the Ionic Liquid [Emim][Im]

Brian W. Ticknor¹, Julie K. Anderson², Bruce A. Fritz³, and Yu-Hui Chiu⁴

Air Force Research Laboratory, Space Vehicles Directorate, Hanscom AFB, Massachusetts, 01731

Porous tungsten emitters of different aspect ratios, produced by a novel electrochemical etching process, are studied by angle-resolved mass spectrometry and retarding potential energy analysis, which provides information on the mechanisms of ion field evaporation and spatial distributions of the emitted ions and droplets. In the present study, the ionic liquid [Emim][Im] (1-ethyl-3-methylimidazolium bis(trifluoromethylsulfonyl)imide) is sprayed from two externally wetted porous tungsten emitters. Near field current and mass flow measurements show that while both emitters operate in a mixed ion-droplet mode, the longer 3 mm emitter has a slower liquid flow rate than the shorter, 2 mm emitter. The mass spectrometric analysis shows that the 3 mm emitter favors the production of smaller ions, while the mass distribution shifts to larger clusters with the use of the 2 mm emitter. The ion energy analysis suggests that all the observed ions and droplets, from both emitters, have energies near that of the emitter potential, seemingly indicating that they are all formed in the neck region of the Taylor cone. The combined near field and mass spectrometry results are consistent with the observation that the shorter emitter supports a larger liquid flow rate to the tip than that produced from the longer emitter, leading to emission that contains a larger fraction of droplets versus ions, and also produces droplets of a larger size.

Nomenclature

I_{sp}	=	specific impulse
m/q	=	mass to charge ratio
V_{ext}	=	total extraction voltage

I. Introduction

IONIC liquids (ILs), or low melting point salts, have attracted considerable attention as propellants for colloid, or electro spray thrusters in spacecraft propulsion applications.¹ The application of a high electric field to the surface of an IL induces a Taylor cone,² which results in emission of charged droplets and ions. The emitted particles are then electrostatically accelerated, producing thrust. The extremely low vapor pressure and high electrical conductivity of this novel class of propellants make them especially well suited for this role. Since the initial proposal by Fernández de la Mora,¹ the electro spray properties of ionic liquids have been extensively studied by numerous groups.³⁻¹³ Additionally, the technology has matured to the point that a colloid thruster is scheduled to fly on the Jet Propulsion Laboratory ST7 Disturbance Reduction Mission later this year.^{4, 14} The propellant of choice for this mission is the IL 1-ethyl-3-methylimidazolium bis(trifluoromethylsulfonyl)imide ([Emim][Im]), which has passed all space exposure tests. Three distinct modes of operation have been identified for IL electro spray thrusters: an ion-only mode (high I_{sp}), a mixed ion-droplet mode, or a pure droplet mode (high thrust).⁴ The dynamics of these differing electro spray modes is controlled by the physical properties of the propellant, particularly the rate of the liquid flow to the emitter tip. Specifically, ion-only electro spray conditions may be achieved by obtaining a low liquid flow rate.^{1, 8} Previous work has shown that the use of porous tungsten emitter may achieve ion-only emission

¹ National Research Council Postdoctoral Associate, Space Vehicles Directorate, AFRL/RVBXT, 29 Randolph Road, Hanscom AFB, MA 01731, AIAA Member.

² Space Scholar, Space Vehicles Directorate.

³ First Lieutenant, Space Vehicles Directorate, AIAA Member.

⁴ Task Scientist, Space Vehicles Directorate, AIAA Member.

20100927141

while still supporting high levels of emitted current.^{15, 16} In the present work, the electro spray properties of [Emim][Im] from two externally wetted porous tungsten emitters with different aspect ratios are studied.

The electrohydrodynamics of a specific electro spray system are governed by emitter characteristics like geometry and material, as well as properties of the IL such as viscosity, surface tension, and conductivity.^{5, 6, 8, 9} Emitter geometries previously studied include capillaries^{1, 10, 14} and externally wetted metallic needles^{3-6, 8, 9, 11-13} and ribbons.^{7, 15-17} The use of capillary emitters allows for very precise control of the liquid flow rate, but is burdened by the need for active pumping and the associated flow controls. Alternatively, externally wetted needles, with passive liquid flow controlled by the capillary action of the liquid along the metal surface, have been shown to support very stable emission in the laboratory, but are limited by relatively small thrust per emitter, $\sim 0.1 \mu\text{N}$.¹⁶ Ribbon emitters, which have a larger surface area than the needles, have been studied for their potential to support larger levels of current emission, but difficulties in controlling the higher flow rate, and thus the electro spray mode, have sometimes prevented their use in the ion-only emission regime.⁷ Constructing an array of emitters is an obvious choice to bolster the total thrust produced,¹⁵⁻¹⁷ but reproducibility creating many identical tips is technologically challenging. Recently, the Space Propulsion Laboratory at the Massachusetts Institute of Technology (MIT) has reported a method for the fabrication of linear arrays of emitters made of porous tungsten.^{15, 16} The method is highly reproducible, and the choice of porous tungsten for the material potentially gives the added advantage of creating high levels of ion-only emission per emitter by allowing liquid flow through the volume of the porous emitter and not just along the surface.

The current work uses angular distribution measurements coupled with mass spectrometric and retarding potential analysis to characterize the electro spray properties of [Emim][Im] externally wetted on two different single emitters of porous tungsten, both with bases of 1 mm, but one 2 mm in length, the other 3 mm. The study of a single emitter is crucial for the future design of arrays, as any interaction of the spray from neighboring emitters has implications for the ideal packing geometry. Additionally, the comparison of the emitters with two different aspect ratios gives insight into the role this specific feature of the geometry has on the flow rate and the corresponding spray properties of the emitters.

II. Experimental

The experimental apparatus has been described in detail previously.³⁻⁷ Briefly, the electro spray thruster source utilizes an externally wetted porous tungsten emitter that is electrochemically etched to produce a sharp tip with a radius of curvature $\sim 5 \mu\text{m}$. Fabrication of the emitters took place at the MIT Microsystem Technology Laboratory and the Space Propulsion Laboratory, utilizing a method developed by Legge *et al.*^{15, 16} Clean porous tungsten (0.5 μm pore size) is coated with an polyimide layer and a layer of photoresist, which is then exposed to UV light for patterning of the desired emitter shape. The photoresist is developed, removing the exposed photoresist and etching the polyimide layer with the shape of the emitter. The excess photoresist is removed with acetone and the sample is baked to cure the polyimide. The tungsten is then electrochemically etched. Areas covered by the patterned polyimide layer are protected, while exposed metal is gradually removed until only the sharpened tip remains. Finally, the emitters are cleaned with piranha solution to remove the remaining polyimide. This single step etching

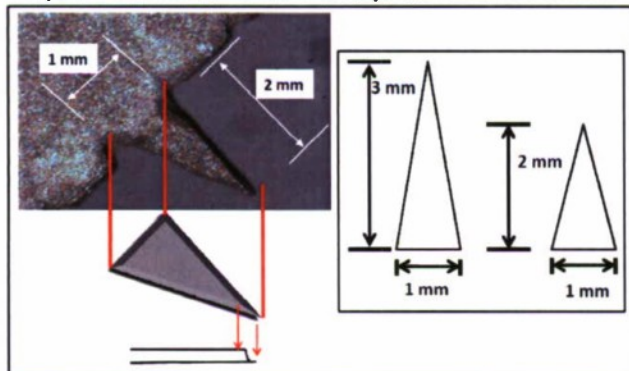


Figure 1. Photograph and schematic depiction of the aspect ratio of the emitters used in this study. The picture on the left emphasizes the asymmetric nature of the emitters produced in the etching process employed.

process leaves an asymmetric emitter, with one side wider than the other. This can be seen in the photograph and schematically in Figure 1. Additionally, even though the etched emitters are cleaned with piranha solution, the possibility exists for contamination by leftover by-product from either the polyimide or the photoresist layers. Evidence for this will be presented below.

Emitter tips of two different aspect ratios were produced and studied in these experiments. The base of both tips is ~ 1 mm, while the lengths are 2 mm and 3 mm respectively. The tip to be studied is wetted with the [Emim][Im] propellant by heating the emitter and then placing drops of liquid on the metal surface until it is saturated. Capillary action and the roughness of the etched metal surface aid the flow of the IL to the emitter

tip. The thruster is aligned with the wider side up, and positioned ~ 0.5 mm from the extractor electrode with a 0.5 mm diameter aperture. The entire source assembly, including the porous tungsten emitter and the extractor electrode, is rotatable with respect to the center axis of the experimental apparatus. Angles of approximately ± 40 degrees are achieved, which allows for the measurement of the ion emission properties of the Taylor cone-jet as a function of emitter angle. The entire ion extraction source is held in vacuum of $\sim 1 \times 10^{-7}$ Torr.

Extraction voltages (V_{ext}) of $\pm 1200 - 1500$ V are used, operated in alternating polarity (AC) mode. Previous work on needle emitters utilizing [Emim][Im] has shown that long term operation of the thruster source in positive polarity can lead to the formation of an electrochemical double layer that throttles the flow of liquid to the emitter tip.^{6, 12} It was found that alternation of the polarity at 1 Hz was sufficient to eliminate such processes, and that methodology is adopted here. The tungsten tip is biased at ± 500 volts, with the extractor biased at $-/+750 - 1000$ V of the opposite polarity. The ± 500 V needle potential is chosen to maximize both mass resolution and ion signal through the mass spectrometer. The total emission current is determined from an electrometer measurement in the emitter power supply biasing circuit, and represents the total amount of current emitted, integrated over all angles. Typical total emission currents observed from the porous tungsten emitters are $\sim 150 - 350$ nAmps, depending on the V_{ext} chosen and the length of the emitter.

The electrospray beam is sampled in the near field by moving one of several possible targets in place. A Faraday cup and a quartz crystal microbalance (QCM; XTM/2, Inficon), both with 6 mm entrance apertures, and a cylindrical lens element for beam transmission are mounted orthogonal to the beam axis on a translation stage, and are interchangeable. The Faraday cup and QCM characterize the electrospray plume by detecting current and mass flow as a function of thruster angle. The ratio of the mass flow to the current allows for an estimation of the average mass per emitted charge, m/q . The third near field target, the cylindrical lens element, allows the beam to pass through a 3 mm diameter aperture, with a solid angle of acceptance of ~ 6 degrees. It is then focused and injected into a quadrupole mass spectrometer for mass analysis. Upon exiting the quadrupole the beam passes through a set of three retarding potential grids and is then detected by an off-axis electron multiplier detector. The angular distribution of the emitted spray is recorded by measuring the mass spectrum as a function of thruster angle. Alternatively, the energy distribution for a selected ion at a specific thruster angle can be measured by recording the depletion of the ion beam at the detector as a function of the voltage applied to the retarding potential analyzer. Both positive and negative ions are studied in this experiment.

III. Results

Figure 2 shows the AC mode Faraday cup and QCM measurements, taken as a function of thruster angle, for both the 3 mm (top) and 2 mm (bottom) emitters at $V_{ext} = 1325$ and 1400 V, respectively. The black squares represent the emitted current registered on the Faraday cup during the positive portion of the AC spray (nA), the black triangles are the detected current during the negative polarity portion of the spray (-nA), and the red circles are the QCM measurements (ng/sec), which here represent a time-averaged combination of the mass flow of the two polarities. Previous work on [Emim][Im] suggests that no significant difference exists in the mass flow readings at the two polarities, so the assumption that the AC mass flow reading approximates the independent DC mass flow readings at positive and negative polarities is reasonable. Current measurements are plotted against the left axis, while the mass flow measurements are plotted against the right axis, and the dashed line is the zero value for both the current and mass flow axes. The current reading for the 3 mm emitter are made while the total emission current is ~ 150 nA, while the 2 mm measurements are made with a total emission

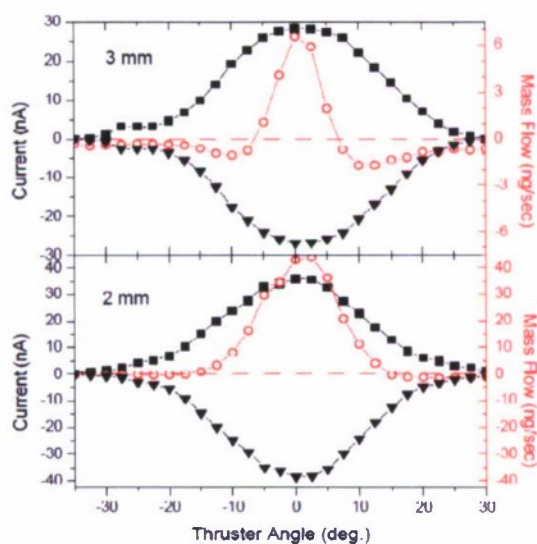


Figure 2. The angular dependence of ion current and mass flow measured with a Faraday cup and QCM meter in the near field with a 3 mm (top) and 2 mm (bottom) emitter. The black squares (+ polarity) and triangles (- polarity) are current measurements (left axis, nA), the red circles are the time averaged combination of mass flow measurements of both polarities (right axis, ng/sec).

current of ~200 nA. The spray of current for both emitter lengths is symmetric and has a similar angular spread, ± 25 degrees to either side of center. The positive and negative polarity components of the spray are approximately equal in magnitude, with maximum readings on the thruster axis of ~30 nA for the 3 mm emitter and ~40 nA for the 2 mm emitter. The QCM readings for the two emitters, however, are fairly different from each other. The 3 mm emitter has a relatively narrow angle of mass flow, $\sim \pm 7.5$ degrees, and a maximum mass deposition rate of 6 ng/sec. The slight negative deposition readings detected at the edges of the mass flow distribution are attributed to ion sputtering processes. The 2 mm emitter, in comparison, has a slightly wider angle of mass flow, $\sim \pm 12.5$ degrees. The peak mass deposition rate here, again located along the thruster axis, is about 40 ng/sec, considerably higher than for the longer emitter. Additionally, no negative deposition is detected here. For the 3 mm emitter, the average m/q of the spray, as estimated from the Faraday cup and QCM measurements, is 22,100 amu for the positive polarity and 23,700 amu for the negative polarity. The 2 mm emitter has an average m/q of 117,000 amu for the positive polarity and 108,500 amu for the negative polarity.

Figure 3 depicts the cation mass spectra as a function of thruster angle from the 2 mm emitter operated in AC mode at $V_{ext} = 1400$ V. Three main mass peaks are observed, corresponding to $Emim^+$ ($n = 0$, 111 amu), $Emim^+([Emim][Im])_1$ ($n = 1$, 502 amu), and $Emim^+([Emim][Im])_2$ ($n = 2$, 893 amu). The spray angle is approximately ± 20 degrees, slightly more narrow than what was seen in the near field current measurements. The overall appearance of the mass spectra is clean, with very little background observed.

Figure 4 shows the positive ion mass spectra as a function of angle for the 3 mm emitter, operated in AC mode with $V_{ext} = 1325$ V. The spray is slightly asymmetric here, extending to 30 degrees on one side of the emitter, and only ~20 degrees to the other side. Two major mass peaks are observed, corresponding to the $n = 0$ ion at 111 amu and the $n = 1$ species at 502 amu. In contrast to the 2 mm emitter, there is no evidence of the $n = 2$ cluster. Additionally, a mass spectral background is seen at small angles which was not present in the 2 mm emitter data. This type of background has been seen in previous experiments and is attributed to the presence of large m/q species, or droplets, in the emitted spray.⁴⁻⁷

Figure 5 is the anion mass spectra plotted as a function of thruster angle for the 2 mm emitter, operated in AC mode at $V_{ext} = 1450$ V. The detected spray angle is fairly wide here, $\sim \pm 25$ degrees, very similar to the spray angle

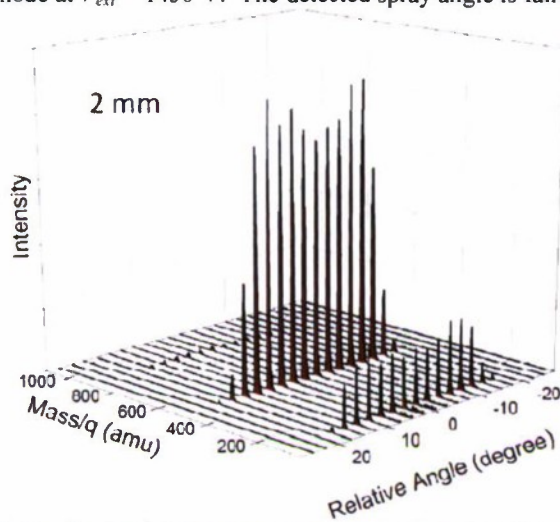


Figure 3. Cation mass spectra for the 2 mm emitter, recorded as a function of thruster angle.

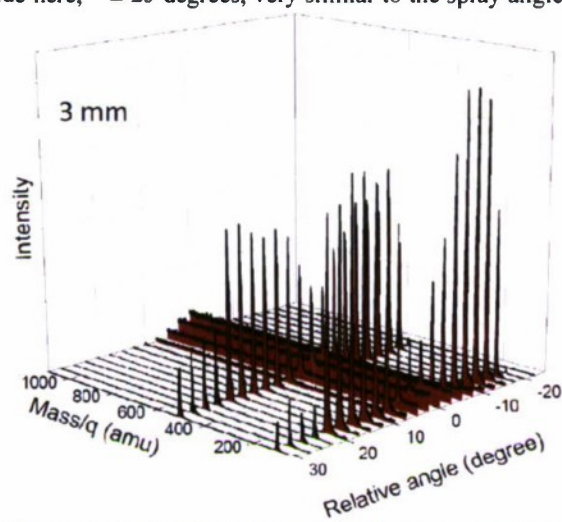


Figure 4. Cation mass spectra for the 3 mm emitter, recorded as a function of thruster angle.

of the negative current detected in the near field with the Faraday cup. Three major ion peaks are present, the Im^- ($n = 0$, 280 amu), $Im^-([Emim][Im])_1$ ($n = 1$, 671 amu), and $Im^-([Emim][Im])_2$ ($n = 2$, 1062 amu), similar to the cation mass spectra observed with the same emitter. However, a couple additional mass peaks are detected. Species are observed at 583 amu and 974 amu. They are currently unassigned, but possibly correspond to impurities remaining from the etching process. A small droplet background can be seen here, at ~ 10 degrees about the thruster center.

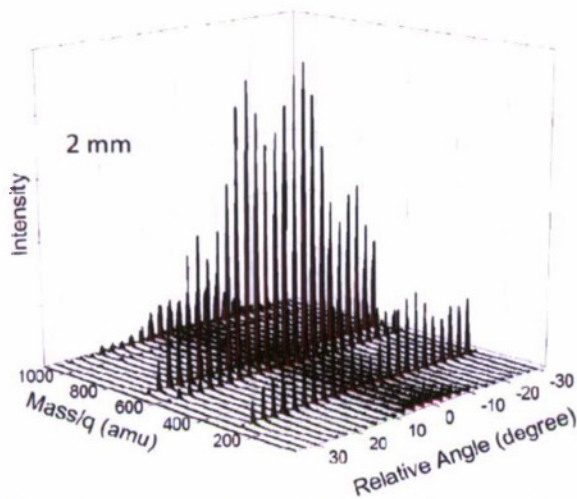


Figure 5. Anion mass spectra for the 2 mm emitter, recorded as a function of thruster angle.

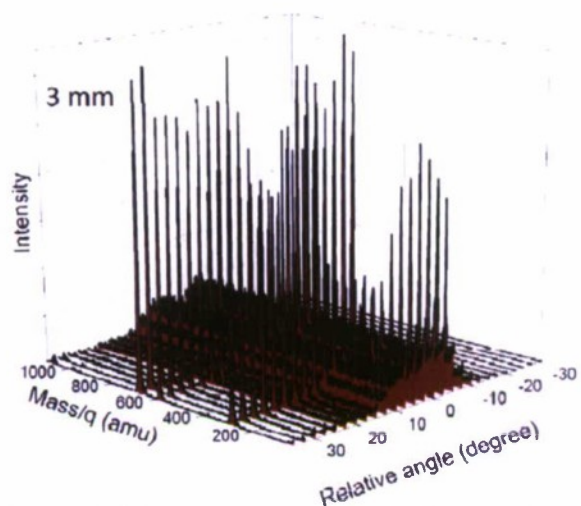


Figure 6. Anion mass spectra for the 3 mm emitter, recorded as a function of thruster angle.

Figure 6 shows the anion mass spectra as a function of thruster angle for the 3 mm emitter in AC mode at $V_{ext} = 1250$ V. Similarly to the cation mass spectra from the 3 mm emitter, the spray is asymmetric, extending past 30 degrees on one side of center and to only 20 degrees on the opposite. Other similarities include the dominance of the $n = 0$ and $n = 1$ peaks, with only a very small amount of the $n = 2$ species. A prominent droplet background is also seen at approximately ± 10 degrees, again similar to that seen for the cations. However, like the 2 mm emitter anion mass spectra, a negatively charged species is observed at 583 amu.

An anion mass spectral trace at a single angle, 12.5 degrees, is shown in Fig. 7. This mass spectrum was taken using the 2 mm emitter. The $n = 0$ and $n = 1$ anion species are most prominent, as mentioned in regards to Fig. 5. The $\text{Im}^+(\text{Emim})[\text{Im}]_2$ peak at 1062 amu is also present, although relatively small. The unassigned peaks at 583 amu and 974 amu are both apparent here, even though the latter is relatively small.

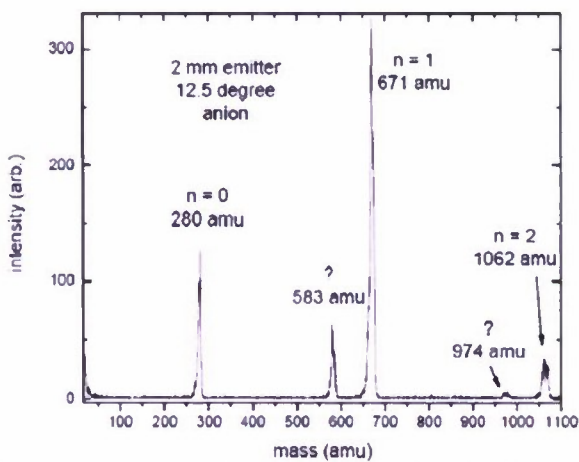


Figure 7. Anion mass spectrum for the 2 mm emitter, recorded a 12.5 degree relative angle.

502 amu) at 0 degree relative angle from the 2 mm emitter is shown in Fig. 8. The open circles represent the average of 3 or 5 scans and the solid line is the smoothed data. The inset shows the corresponding energy distribution of the selected ion, obtained by plotting the derivative of the smoothed retarding potential curve. The ion energy distribution shows a single, fairly broad peak, centered at ~ 475 eV, close to the 500 V emitter potential.

The retarding energy potential curve measured for mass-selected $\text{Emim}^+(\text{Emim})[\text{Im}]_1$ cation ($n = 1$,

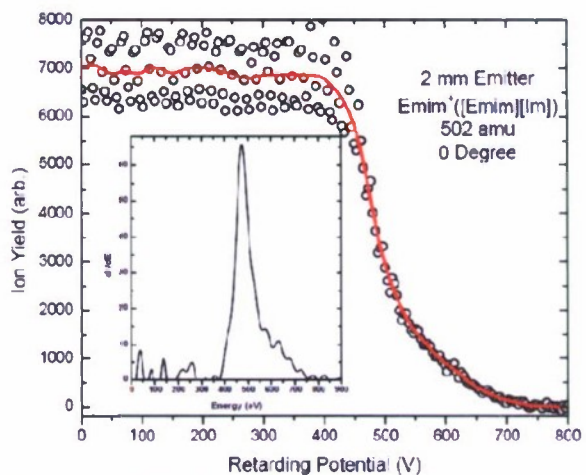


Figure 8. The 2 mm emitter retarding potential curve for $\text{Emim}^+(\text{Emim})[\text{Im}]_1$ at 0 degrees. The inset is the corresponding energy distribution.

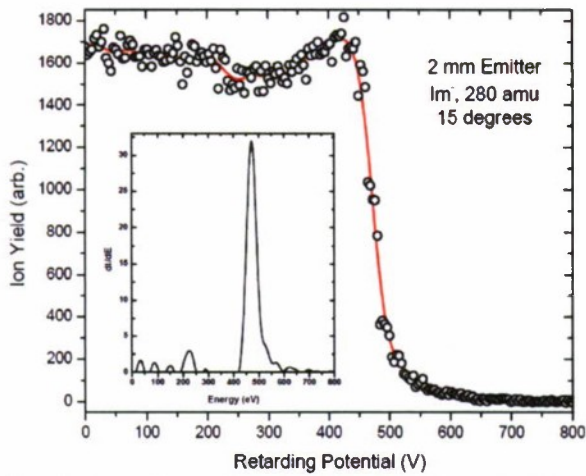


Figure 9. The 2 mm emitter retarding potential curve for Im^- at 15 degrees. The inset is the corresponding energy distribution.

Figures 9 and 10 show the retarding potential curves and the corresponding ion energy distributions for the mass selected Im^- ($n = 0$, 280 amu) anion and the negatively charged 583 amu species from the 2 mm emitter, both measured at a relative thruster angle of +15 degrees. The energy distributions of both ions show one sharp peak centered at ~ 475 eV.

Figures 11 – 13 are retarding potential curves and ion energy distributions for various ions emitted from the 3 mm thruster tip. The Emim^+ ($n = 0$, 111 amu) cation, at +35 degrees, is shown in Fig. 11. A single peak is observed here in the ion energy distribution, at 500 eV, right at the emitter potential. The retarding potential curve and ion energy distribution shown in Fig. 12 is the Im^- ($n = 0$, 280 amu) anion from the 3 mm emitter, at a relative angle of 0 degrees, the center of the spray. One peak is present in the energy distribution, centered at ~ 470 eV. The retarding potential of high m/q positive

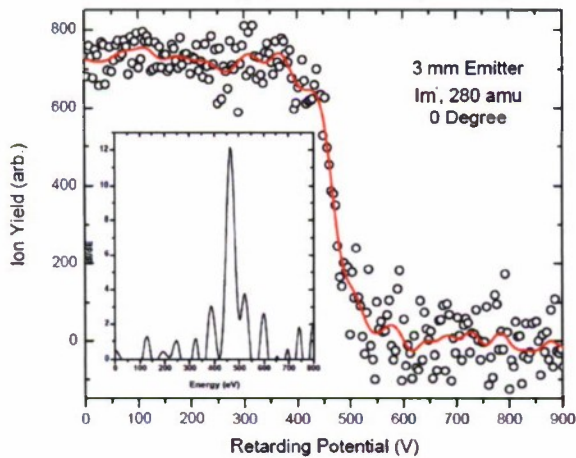


Figure 12. The 3 mm emitter retarding potential curve for Im^- at 0 degrees. The inset is the corresponding energy distribution.

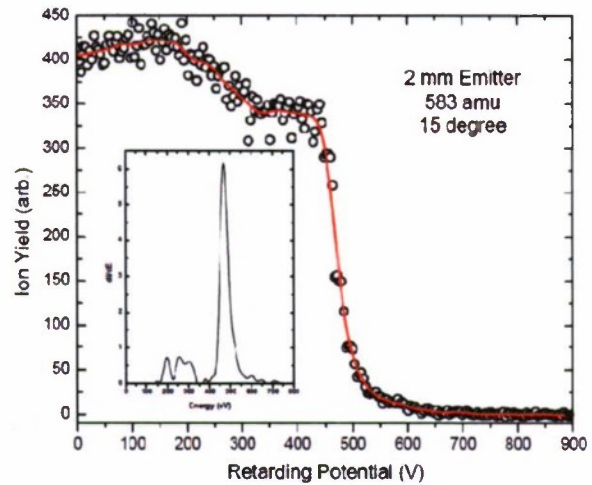


Figure 10. The 2 mm emitter retarding potential curve for the 583 amu species at 15 degrees. The inset is the corresponding energy distribution.

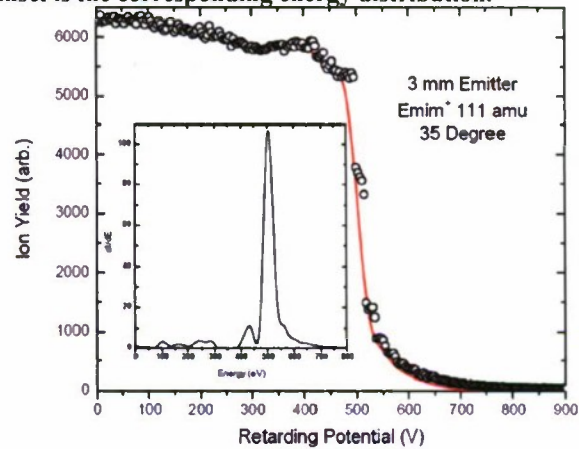


Figure 11. The 3 mm emitter retarding potential curve for Emim^+ at 35 degrees. The inset is the corresponding energy distribution.

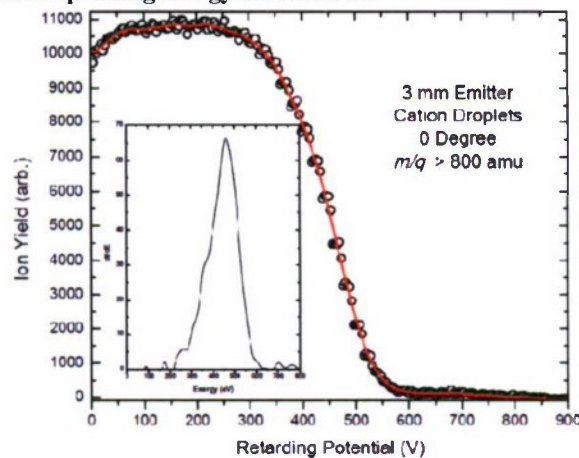


Figure 13. The 3 mm emitter retarding potential curve for high m/q cation particles at 0 degrees. The inset is the corresponding energy distribution.

species produced at 0 degree relative angle is depicted in Fig. 13. The curve is collected with the quadrupole mass spectrometer set in an rf-only mode in which the amplitude is set to only pass high m/q particles ($> \sim 800$ amu). Filtering out the low mass ions out provides a method for both detecting the presence and analyzing the energy of high m/q species (droplets). The energy distribution has a single, very broad feature, peaked at ~ 460 eV. Significant ion intensity is detected at energies as low as 300 eV, however. The retarding potential curves and ion energy distributions shown here are representative examples. All ions from both emitters, at both polarities, at multiple angles, that were detected in enough intensity were measured in these experiments.

IV. Discussion

The combination of the near field current and mass flow measurements with the far field mass spectral data suggest that both the 2 mm and 3 mm emitters operate in a mixed ion-droplet emission mode. Substantial differences in the emission from the two emitters do exist, however, and careful examination of data gives some insight into the similarities and differences with which the thrusters operate. First, as mentioned above, the 3 mm emitter was operated at a lower V_{ext} than the 2 mm one, 1325 V versus 1400 V respectively. The V_{ext} chosen is typically the lowest voltage at which stable emission is achieved. Previous work on externally wetted emitters has shown that the emission mode of a single emitter can be shifted by changing V_{ext} , which in turn affects the rate of liquid transport to the tip.⁷ The difference in V_{ext} for the two emitters here likely indicates a similar shift in propellant flow rate and subsequently in the emission mode of the thruster.

Some other notable disparities between the two different length emitters are evident from the near field current and mass flow measurements in Fig. 2. The 3 mm emitter has a smaller magnitude of emitted current as measured by the Faraday cup than the 2 mm emitter for both the positive and negative polarities, again indicative of differences in the liquid flow rates at which the emitters are operating. The 2 mm emitter, with a higher V_{ext} and higher current measurements, supports a higher liquid flow rate to the tip and thus a different emission mode.

This conclusion is supported by the near field mass flow measurements, depicted with red circles in Fig. 2. As mentioned above, the 3 mm emitter shows some positive mass deposition, peaked on axis, as well as negative mass flow at larger angles, where current emission is still high. This is attributed to sputtering of the crystal surface by fast moving ions, which carry measureable charge but no appreciable mass. This type of mass deposition has been seen previously in our lab from externally wetted needle emitters and indicates a mixed ion-droplet mode of operation, in which droplet emission predominates in the center, with ions favored at high angles.^{4,6} The estimate of the average m/q of emitted particles, $\sim 22,000$ amu for this emitter, is also very similar to that observed previously from needle emitters, and helps to confirm the liquid flow rate and the emission mode under which this thruster is operating.

The mass flow measured from the 2 mm emitter, in the bottom trace of Fig. 2, shows a large amount of mass deposition on axis, and no negative deposition. This is similar to the emission seen previously from externally wetted ribbon emitters, which were shown to accommodate higher liquid flow rates than the needles.⁷ The estimate of the average m/q of emitted particles of $> 100,000$ amu gives further evidence that the length of the emitter affects the liquid flow rate and the emission mode. In the case of the 2 mm emitter, the thruster is still operating in a mixed ion-droplet mode, but the higher liquid flow rate shifts the emission mode and leads to a correspondingly larger amount of droplets relative to ions. The mass spectral data, discussed below, agrees with this analysis.

The angle resolved mass spectra for the 3 mm emitter, shown in Figs. 4 (cation) and 6 (anion), are dominated by the $n = 0$ and $n = 1$ ions, seen in approximately equal intensity in both the cation and anion data. As mentioned above, the spray is somewhat asymmetric, but the spray angles at which ions are detected roughly correspond to the angles at which current was detected in the near field. Additionally, at small angles about the thruster center, a background is observed throughout the mass spectra and the ion signals are somewhat depleted. This feature has been previously observed and attributed to the presence of large m/q species, or droplets, that are not completely filtered out by the quadrupole and thus reach the detector.^{4,6,7} The angular distribution of this background closely corresponds to the thruster angles at which mass deposition is measured on the QCM, helping to confirm its assignment as being due to the presence of droplets in the spray. In this case, the Taylor cone formed at the tip of the emitter stretches out to form a jet, and the jet can then pinch off and emit charges in the form of large droplets, rather than as individual ions. At the larger angles, where no droplet background and no mass deposition is observed, ion field evaporation dominates and mainly discrete ionic species are detected. The appearance of the mass spectra from the 3 mm emitter very closely mirrors that observed previously in our laboratory from externally wetted needle emitters, as the near field data did.^{4,6} The emission mode is one of mixed droplets and ions, with a relatively slow liquid flow rate, but not low enough to fully enter an ion-only electrospray regime.

Compared to the 3 mm emitter data, the angle resolved mass spectra for the 2 mm emitter (Figs. 3, cation, and 5, anion), suggest a higher rate of propellant flow, reminiscent of previous experiments in our laboratory utilizing externally wetted ribbon emitters.⁷ For the anions, the angular distribution of the detected ions is similar to that measured for the current in the near field with the Faraday cup, while the angular distribution of the cations appears narrower than might be expected in comparison to the near field measurements. The exact reason for this discrepancy is unknown, but something as simple as the setting of the detector voltage may be to blame, preventing the observation of the small ion signals at large angles. In mass spectra for both polarities, the $n = 0$ ion is observed, but $n = 1$ is now clearly the dominant species, and the $n = 2$ cluster is also detected. Thermal stability of these species has been predicted to decrease as cluster size increases, so the enhancement in intensity of the $n = 1$ and $n = 2$ clusters suggests that some mechanism must exist that helps to quench excess internal energy. Evaporative cooling, where particles boil off either charged or neutral species until their internal energy is below the threshold for cluster stability, has been invoked previously to explain the observation of the larger ionic clusters.⁶ Although this experiment does not reveal the precise cooling mechanism that occurs, the mass spectral data certainly indicates that the cooling process is more efficient in the spray from the 2 mm emitter as opposed to the 3 mm one. An enhancement of this effect would also be consistent with thruster conditions that favor the formation of droplets, as the dissociation of large particles would be able to quench a greater level of internal energy as compared to smaller droplets. The cooling process is thus favored by the higher flow rate conditions that occur with the shorter emitter.

A conspicuous feature of the mass spectra from the 2 mm emitter mass spectra is the lack of the mass spectral background, due to droplets, that was seen from the longer emitter. The absence of this background seems counter-intuitive to the claim that the shorter emitter is actually supporting a higher liquid flow rate and thus producing larger droplets. However, the discrepancy can be explained by the detection efficiency of the droplets as a function of size. As noted above, the average m/q of the particles emitter from the 3 mm thruster is $\sim 22,100$ amu and $\sim 23,700$ amu, respectively, for the positive and negative polarities. The average m/q for the 2 mm thruster, however, is $\sim 117,000$ and $\sim 108,500$ amu, respectively. The detection efficiency of these particles depends on the energy per charge, however, not the m/q . Because smaller droplets are expected to have a higher energy per charge than larger droplets, they will be detected more efficiently. Thus the background observed in the mass spectra is more prominent when smaller droplets are produced, as is the case in the 3 mm emitter.

One interesting similarity found in the anion mass spectra of both the 2 and 3 mm emitters is the presence of the unassigned peak at 583 amu. The 2 mm emitter additionally has a small mass peak at 974 amu, which likely corresponds to the 583 amu species clustered with an [Emim][Im] neutral ion pair. These peaks can be clearly seen in Fig. 6. In previous electrospray experiments utilizing [Emim][Im] this peak has not been observed,^{6, 7, 11, 15, 16} which suggests that it may be due to an impurity, possibly remaining from etching process employed with the novel porous tungsten material. The fact that it occurs in both the 2 and 3 mm emitters, which have different liquid flow rates and emission modes, provides evidence that the origin of this peak is not related to the specific details of the electrospray dynamics. To investigate the possibility that an impurity may be responsible, testing of a second batch of porous tungsten emitters was conducted, and the 583 amu peak was again observed. Thorough, repeated washing of the emitters in water, acetone, and ethanol in a sonicating bath, was then completed to remove any remaining contamination. After careful washing, the 583 amu peak was still seen, but its intensity has decreased tremendously, as would be expected for an impurity that cleaning would remove. Although a definitive assignment of the peak is not made here, the mostly likely explanation is that of contamination from the etching process.

The suggestion here of a mixed ion-droplet emission mode similar to that observed from externally wetted metallic emitters largely agrees with previous results in our lab,³⁻⁷ but the groups of Lozano^{11, 15, 16} and de la Mora^{8, 9} have reported ion only emission from a variety of different types of emitters. The exact geometry of the emitter tip is now understood to be important.^{8, 9} A small radius of curvature of the tip limits the liquid flow rate and favors ion-only emission, while larger tips accommodate greater liquid flow and can favor a mixed droplet-ion emission regime or even droplet only emission. Droplet only emission has also been observed from high propellant flow rates using capillary emitters, where the flow rate is actively and accurately controlled.¹⁴ The precise emitter geometry can account for some of the discrepancies between emission modes previously observed among various laboratories. In this case, however, the emitters used in these experiments were produced in the MIT Microsystem Technology Laboratory and the Space Propulsion Laboratory using the procedure developed by Legge *et al.* that was reported to produce emitters that operated in an ion-only emission mode.^{15, 16} The exact cause of the difference in the emission mode observed here versus the previous work at MIT is unclear. However, subsequent investigations in our laboratory using another porous tungsten emitter fabricated by a similar procedure in the MIT lab have revealed evidence of ion-only emission, with no measurable mass deposition recorded. Thus the mixed ion-droplet mode observed here may be the result of local geometric tip features unique to these particular emitters. Another difference may occur from the wetting of the porous tungsten. The electrospray properties maybe be significantly

different if the emitter tip has a standing layer of liquid on the surface which flows to the tip, versus liquid filling the pores and flowing internally through the porous metal. The wetting and liquid flow mechanisms are not well characterized here, and additional experiments are planned.

Ion energy distributions are a useful tool to determine the point of origin for emitted ions. Ion energies very near the applied emitter voltage typically indicate that they are formed in the neck region of the Taylor cone where the maximal normal electric field occurs, generally directly by field evaporation from the liquid surface. Ion energies much below the emitter potential typically mean that the particle is formed in the jet region of the Taylor cone, where the cone pinches off to form droplets. Downstream in the jet ohmic losses occur, and thus the energy of particles emanating from this region will be lower.⁶ Particles with this lower energy can include droplets, ions emitted from the jet, or ions formed from the dissociation of droplets. Previous work has shown that in a mixed ion-droplet emission mode, droplets, usually found on axis, do indeed have energies lower than the emitter potential. Ions at larger angles generally have energies near the emitter potential, but on axis ions have been observed at much lower energies, suggesting their genesis is in the jet region or from droplet dissociation.^{4, 6, 7} Higher liquid flow rates, with correspondingly larger droplets, generally favored the production of ions in the jet region.

The retarding potential curves and associated ion energy distributions presented in Figs. 8 – 13 show perhaps surprisingly similar results for the 2 and 3 mm emitters. For the 2 mm emitter, the single peak in the energy distribution for the Emim^+ ($[\text{Emim}][\text{Im}]$), ($n = 1$, 502 amu) cation at a thruster angle of 0 degrees (Fig. 8) comes at ~ 475 eV. The peak is broad, but an ion energy so close to the voltage applied to the emitter indicates the ions are formed at the neck of the Taylor cone, where few ohmic losses occur. The same is true of the Im^- ($n = 0$, 280 amu) anion energy distribution at an angle of 15 degrees in Fig. 9. A single, fairly sharp peak, centered at ~ 475 eV, shows that this ion also is formed in the neck region of the Taylor cone. The energy distribution for the 583 amu anion peak, also at 15 degrees, in Fig. 10 appears very similar. The single peak centered at ~ 475 eV again suggests an origin in the Taylor cone neck region. Additionally, the similarity of the energy distribution of the 583 amu anion to the $n = 0$ anion at the same angle supports the assumption that it is due to an impurity, presumably one on the surface that is picked up and carried by the flow of the liquid to the emitter tip. A dramatically different appearance to its energy distribution may have suggested that the presence of this species was due to a previously unobserved electrospray emission mode unique to these novel porous tungsten emitters, but this result suggests that this interpretation is unlikely.

The energy distributions of ions from the 3 mm emitter are similar to those of the 2 mm emitter. In the energy distribution of the Emim^+ cation ($n = 0$, 111 amu) at a thruster angle of 35 degrees in Fig. 11, the single peak centered at ~ 500 eV indicates that these ions formed in the neck region of the Taylor cone. The Im^- ($n = 0$, 280 amu) anion at a 0 degree angle, in Fig. 12, also has a single major peak, at ~ 470 eV, again close to the emitter potential and indicative of its formation in the neck region. In fact, the measured ion energy distributions for all ions measured, from both emitters at both polarities, and at large and small relative angles, are found to be $\sim 460 - 500$ eV, indicating that all the observed ions are formed in the Taylor cone neck. Even the energy distribution of positively charged large m/q droplets from the 3 mm tip, in Fig. 13, is peaked at ~ 460 eV. The distribution is very broad, and contains features at energies of 300 eV and below. But the presence of the majority of the ion signal in the range of 460 eV is puzzling. Previous experiments have consistently found the energy of high m/q particles to be well below 400 eV, sometimes as low as 250 eV.^{4, 6, 7} Again, this is due to the ohmic losses that occur when the cone stretches out into a jet, which pinches off to form droplets. Likewise, ions emitted on axis, co-linear with the droplets, have previously been found to have energies lower than 450 eV, and often down to 300 eV, as would be expected for ions formed at the jet or which dissociate from droplets that are formed at the jet. The absence of these low energy ions, especially on axis and especially for the higher flow rate emitter, is surprising.

There are several possible explanations for these seeming anomalous results of the ion energy measurements. First, regarding the droplet energy distribution in Fig. 13, the true droplet energy may be the features seen on the low energy side of the peak. High mass ions, smaller than droplets but still beyond the mass resolving range of the quadrupole (in high pass mode, > 800 amu), could be contaminating the signal. Significant amounts of unresolved heavy ions, formed, like the lower mass ions, at 470 – 500 eV, may obscure the true droplet energy. A second possibility is that the particles are formed with extremely low energy, and are thus filtered out by the 200 V float applied to the quadrupole. This could occur by the formation of an extremely long Taylor cone-jet, which would suffer from significant ohmic losses. If the energy of the droplets or ions emitted from the end of the jet dropped below 200 V they would not be detected. A third possibility is the formation of a Taylor cone with a very short jet region, which would minimize ohmic losses. The cone could conceivably still pinch off to form droplets, as with the longer jet, but the energy of the droplets, as well as any ions produced from their dissociation, would have energies close to that of the emitter potential. Whether the use of the porous tungsten material and/or the emitter

geometry produced by the etching process employed somehow favors an extremely short cone-jet is unclear. More work with new emitters is presently under way in the laboratory.

V. Conclusion

Angle resolved current, mass flow, and mass spectrometric measurements for the IL [Emim][Im] electro sprayed from two externally wetted porous tungsten emitters are reported. Tip geometry is well known to have specific and often dramatic effects on the electro spray properties of externally wetted emitters. Here, emitter tips with lengths of 2 and 3 mm, both with 1 mm bases, are studied to determine any differences in their electro spray properties arising from their aspect ratios. The experiments showed that distinct emission modes do exist from the two emitters, likely governed by the flow rates of liquid propellant to the emitter tip.

The 3 mm emitter operated in a mixed ion-droplet mode reminiscent of that seen previously in our laboratory for externally wetted needle emitters. In the near field, the measured current emission extended to ~25 degrees about either side of center, while the mass flow measurements were peaked on the thruster axis, indicating droplets are formed. The spray at high angles, where current is detected with no measured mass deposition, contains mainly ions. This is confirmed by the angle resolved mass spectrometric analysis at both positive and negative polarities. The $n = 0$ (Emim^+ and Im^-) and $n = 1$ ($\text{Emim}^+([\text{Emim}][\text{Im}])_1$ and $\text{Im}^-([\text{Emim}][\text{Im}])_1$) clusters dominate the mass spectrum. The ions are most intense at high angles, while a mass spectral background, attributed to the presence of large m/q droplets, is found on axis.

The spray from the 2 mm emitter also contains a mix of ions and droplets, but the emission mode is clearly different, likely due to the shorter emitter supporting a faster rate of liquid flow to the tip. The near field measurements show measured mass flow at much wider angles, almost as wide as the measured current, which suggests a wider distribution of droplets, and a higher liquid flow rate, as compared to the longer emitter. The appearance of the mass spectra agree with this interpretation as well. In both polarities the $n = 1$ species dominates, and the $n = 2$ clusters are also evident. The shift in the mass distribution to larger clusters, which are less thermally stable than the smaller species, is likely due to more efficient evaporative cooling that is favored in the higher flow rate, larger droplet electro spray regime.

For both emitters an anionic species, which had not been previously observed from electro sprayed [Emim][Im], was detected at 583 amu. The peak remains unassigned, but is likely due to impurities remaining from the etching process, as careful cleaning of an emitter etched in a similar manner significantly reduced the relative size of the peak in the mass spectrum.

The energy distributions measured for cations and anions at both polarities show that all the ions measured in the experiment have energies very close to the emitter potential, suggesting they are all formed at the neck of the Taylor cone, where no ohmic losses occur. Even the energy distribution measured for high m/q droplets was peaked nearly at the emitter potential. This behavior deviates significantly from previous work in our lab on both externally wetted needles and ribbons. The exact reason for this discrepancy is not clear, but the specific geometry of these porous tungsten tips may play a role, possibly causing the formation of a Taylor cone with a very short jet. Droplets are still formed, but ohmic losses are minimized, and thus the droplet energies, as well as any ions formed in the jet region, are detected with energies near the emitter potential, making them nearly indistinguishable from ions produced in the neck region.

The initial tests of porous tungsten emitters presented here definitively show that the length of the emitter dramatically influences the flow rate of the liquid propellant to the emitter tip, and thus the emission mode in which the tip operates. Both emitters operate in a mixed ion-droplet mode, but the longer 3 mm tip has a slower flow rate that favors smaller ions and droplets, while the shorter 2 mm emitter supports a greater rate of liquid flow and favors the production of larger droplets and ionic clusters. Future work in the lab will include more studies of porous tungsten tips, including careful studies of the wetting properties, and their affect on the emission modes.

Acknowledgments

We wish to thank Dan Courtney and Paulo Lozano of the MIT Space Propulsion Laboratory for preparing the porous tungsten emitters used in this work. This research was performed while B. W. Ticknor held a National Research Council Research Associateship Award at the AFRL/Space Vehicles Directorate. J. Anderson thanks the AFRL/Space Vehicles Directorate Space Scholar program. Support for this work by AFOSR through task 2303ES02 (Program Manager: Michael Berman) is gratefully acknowledged.

References

- ¹Romero-Sanz, I., Bocanegra, R., Fernandez de la Mora, J., and Gamero-Castano, M. "Source of heavy molecular ions based on Taylor cones of ionic liquids operating in the pure ion evaporation regime." *Appl. Phys.* Vol. 94, 2003, p. 3599.
- ²Fernandez de la Mora, J. "The Effect of Charge Emission From Electrified Liquid Cones." *J. Fluid Mech.* Vol. 243, 1992, p. 564.
- ³Chiu, Y., Austin, B. L., Dressler, R. A., Levandier, D., Murray, P. T., Lozano, P., and Martinez-Sanchez, M. "Mass Spectrometric Analysis of Colloid Thruster Emission from Selected Propellants," *J. Prop. Power* Vol. 21, 2005, p. 416.
- ⁴Chiu, Y., and Dressler, R. A. "Ionic Liquids for Space Propulsion," *Ionic Liquids IV: Not Just Solvents Anymore*. American Chemical Society, Washington DC, 2007, p. 138.
- ⁵Chiu, Y., Gaeta, G., Heine, T. R., and Dressler, R. A. "Analysis of the Electrospray Plume from the EMI-Im Propellant Externally Wetted on a Tungsten Needle," *42nd AIAA/ASME/ASEE Joint Propulsion Conference & Exhibit*. Scareamento, CA, 2006, pp. AIAA 2006-5010.
- ⁶Chiu, Y., Gaeta, G., Levandier, D., Dressler, R. A., and Boatz, J. A. "Vacuum Electrospray Ionization Study of the Ionic Liquid, [Emim][Im]," *Int. J. Mass Spectrom.* Vol. 265, 2007, pp. 146-158.
- ⁷Ticknor, B. W., Miller, S.W., and Chiu, Y.H. "Mass Spectrometric Analysis of the Electrospray Plume from an Externally Wetted Tungsten Emitter," *45th AIAA/ASME/SAE/ASEE Joint Propulsion Conference and Exhibit*. Denver, Colorado, 2009, pp. AIAA 2009-5088.
- ⁸Castro, S., and Fernandez de la Mora, J. "Effect of Tip Curvature on Ionic Emissions from Taylor Cones of Ionic Liquids from Externally Wetted Tungsten Tips," *J. Appl. Phys.* Vol. 105, 2009, pp. 034903-1.
- ⁹Castro, S., Larriba, C., Mora, J. F. d. I., Lozano, P., Sumer, S., Yoshida, Y., and Saito, G. "Effect of liquid properties on electrosprays from externally wetted ionic liquid ion sources," *J. Appl. Phys.* Vol. 102, No. 9, 2007, p. 094310.
- ¹⁰Garoz, D., Bueno, C., Larriba, C., Castro, S., Romero-Sanz, I., Mora, J. F. d. I., Yoshida, Y., and Saito, G. "Taylor cones of ionic liquids from capillary tubes as sources of pure ions: The role of surface tension and electrical conductivity," *J. Appl. Phys.* Vol. 102, No. 6, 2007, p. 064913.
- ¹¹Lozano, P. "Energy Properties of and EMI-Im Ionic Liquid Ion Source," *J. Phys. D: Appl. Phys.* Vol. 39, 2006, p. 126.
- ¹²Lozano, P., and Martinez-Sanchez, M. "Ionic Liquid Ion Sources: Suppression of Electrochemical Reactions Using Voltage Alternation," *J. Colloids Interface Sci.* Vol. 208, 2004, p. 149.
- ¹³Lozano, P., and Martínez-Sánchez, M. "Ionic liquid ion sources: characterization of externally wetted emitters," *J. Colloid Interface Sci.* Vol. 282, No. 2, 2005, pp. 415-421.
- ¹⁴Gamero-Castano, M., Hruby, V., Spence, D., Demmons, N., McCormick, R., Gasdaska, C., and Falkos, P. "Micro Newton Colloid Thruster for ST7-DRS Mission," *39th AIAA/ASME/SAE/ASEE Joint Propulsion Conference and Exhibit*. Huntsville, Alabama, 2003, pp. AIAA 2003-4543.
- ¹⁵Courtney, D. G., Lozano, P. C. "Porous Ionic Liquid Ion Source Fabrication Refinements and Variable Beam Energy Experiments," *45th AIAA/ASME/SAE/ASEE Joint Propulsion Conference*. Denver, CO, 2009, pp. AIAA 2009-5087.
- ¹⁶Legge Jr., R. S., Lozano, P., and Martinez-Sanchez, M. "Fabrication and Characterization of Porous Metal Emitters for Electrospray Thrusters," *30th International Electric Propulsion Conference*. Florence, Italy, 2007, pp. IEPC-2007-145.
- ¹⁷Lozano, P., Glass, B., and Martinez-Sanchez, M. "Performance Characteristics of a Linear Ionic Liquid Electrospray Thruster," *29th International Electric Propulsion Conference*. Princeton, New Jersey, 2005, pp. IEPC-2005-192.